mathematics

MDPI

Article

Adaptive Fixed-Time Prescribed Performance Command-Filtered Control for Nonlinear Systems with Unknown Control Gains and Actuator Faults

Hadil Alhazmi [1], Mohamed Kharrat [2], Asma Al-Jaser [1] and Paolo Mercorelli [3,*]

[1] Department of Mathematical Sciences, College of Science, Princess Nourah Bint Abdulrahman University, P.O. Box 84428, Riyadh 11671, Saudi Arabia; hnalhazmi@pnu.edu.sa (H.A.); ajaljaser@pnu.edu.sa (A.A.-J.)
[2] Mathematics Department, College of Science, Jouf University, Sakaka 72388, Saudi Arabia; mkharrat@ju.edu.sa
[3] Institute for Production Technology and Systems, Leuphana University of Lueneburg, 21335 Lueneburg, Germany
* Correspondence: paolo.mercorelli@leuphana.de

Abstract

This paper investigates the adaptive prescribed performance fixed-time control problem for uncertain strict-feedback nonlinear systems in the presence of unknown control coefficients and actuator faults. A switching-based control strategy is developed to address the uncertainty in control coefficients, where adaptive parameters are adjusted online according to design requirements. To regulate the transient and steady-state behavior, a fixed-time prescribed performance function is incorporated into the control design, ensuring that the tracking error evolves within predefined bounds. The command filter technique is employed to simplify the backstepping procedure and avoid the issue of complexity growth, while filter-induced errors are compensated using auxiliary signals. Rigorous Lyapunov analysis establishes that all closed-loop signals remain bounded and that the tracking error converges to a small neighborhood of zero within a fixed time, independent of initial conditions. The effectiveness of the proposed method is demonstrated through numerical simulations and a practical example.

Keywords: nonlinear systems; unknown control coefficients; actuator faults; adaptive control; command filters

MSC: 93C10; 93C40; 37N35

Academic Editor: Dawei Gong

Received: 24 March 2026
Revised: 6 May 2026
Accepted: 18 May 2026
Published: 21 May 2026

1. Introduction

The design of tracking controllers for nonlinear systems in the presence of uncertainties has been a central topic in control theory. In practical applications, uncertain parameters and external disturbances are unavoidable, which makes robust controller design both challenging and essential [1–4]. Among various approaches, adaptive control has attracted significant attention due to its ability to adjust online and compensate for unknown system dynamics. When combined with the recursive backstepping framework, adaptive techniques provide a systematic methodology for handling nonlinear systems with hierarchical structures [5–7]. Despite its effectiveness, the backstepping approach suffers from a major limitation, namely the need to repeatedly compute virtual control laws and their derivatives at each design step, leading to the well-known issue of "computational explosion." To address this drawback, the dynamic surface control (DSC) technique was

introduced, where low-pass filters are employed to approximate the derivatives of virtual control signals, thereby reducing computational complexity. However, the filtering process introduces approximation errors that may degrade tracking performance if not properly compensated [8–10]. To further improve performance, command filter-based adaptive control has been developed. In this framework, virtual control signals are processed through command filters to generate smooth derivative estimates, while additional compensation mechanisms are incorporated to mitigate filtering-induced errors [11]. This approach effectively balances implementation simplicity and control accuracy, and has been widely studied in recent literature [12,13]. For example, command filter-based adaptive finite-time control has been proposed for uncertain nonlinear systems to achieve fast convergence [14], while extensions to systems with actuator constraints, large-scale structures, and switched dynamics have also been reported [15–17].

Previous research on adaptive control has generally been conducted under the assumption that the control coefficients are known and constant, often normalized to unity. However, in practical scenarios, control coefficients are typically uncertain and may vary with time [18]. This uncertainty introduces significant challenges in controller design and can degrade the performance of conventional fixed-time control strategies. Moreover, system nonlinearities, actuator faults, and external disturbances may further induce unknown variations in the control coefficients, which must be properly addressed to ensure reliable system performance. Recent research has made notable progress in this direction [19,20]. For example, adaptive control schemes have been developed for nonlinear systems with actuator faults and unknown control directions using command filters, ensuring stable performance under fault conditions [21]. For systems with input nonlinearities and unknown virtual control coefficients, adaptive control strategies have been proposed to achieve robust tracking performance [22]. In addition, adaptive output-feedback event-triggered tracking control has been introduced for nonlinear systems with unknown control coefficients, improving system response while reducing communication load [23]. Furthermore, adaptive finite-time prescribed performance control has been investigated for stochastic nonlinear systems with unknown virtual control coefficients, providing guaranteed performance within a finite-time framework [24]. Despite these advancements, the integration of unknown control coefficients, actuator faults, and prescribed performance within a fixed-time control framework remains an open and challenging problem.

The control strategies discussed above typically ensure convergence as time approaches infinity. However, in many practical systems, it is desirable for the system states to reach the desired equilibrium within a finite time. Finite-time control methods provide faster convergence and improved robustness compared to asymptotic approaches [25–27]. Nevertheless, a key limitation of finite-time control is its dependence on initial conditions, as the settling time varies with different initial states. To overcome this limitation, fixed-time control has been introduced, where the convergence time is independent of initial conditions and can be explicitly determined by design parameters [28]. In recent years, significant progress has been made in this area [29,30]. For example, adaptive fixed-time command-filtered control has been proposed for nonlinear systems with input quantization, achieving fast convergence under quantization effects [31]. For systems with time-varying full-state constraints and actuator hysteresis, adaptive fuzzy fixed-time tracking control has been developed to ensure robust performance [32]. In addition, prescribed performance-based fixed-time control schemes have been investigated using dynamic event-triggered mechanisms to balance tracking performance and communication efficiency [33]. Furthermore, fixed-time event-triggered adaptive control has been designed for uncertain nonlinear systems with full-state constraints, ensuring convergence within a fixed time while reducing communication load [34]. Despite these developments, the integration of

fixed-time control with prescribed performance, unknown control coefficients, and actuator faults remains insufficiently addressed, which motivates the present study.

To ensure that system behavior remains within predefined acceptable limits, prescribed performance control (PPC) has been extensively studied for nonlinear systems [35]. This framework guarantees that the tracking error evolves within a predefined performance envelope, ensuring that both transient and steady-state behaviors satisfy prescribed bounds. Specifically, PPC constrains the overshoot, convergence rate, and steady-state accuracy, thereby providing predictable and reliable system responses. Recent studies have further extended PPC in various directions [36–38]. For example, fixed-time prescribed performance control has been proposed for nonlinear systems with unknown time-varying parameters, ensuring convergence within a preassigned time bound [39]. For switched high-order nonlinear systems, fuzzy adaptive quantized tracking control has been developed under a fixed-time prescribed performance framework to address switching and input quantization effects [40]. In addition, PPC-based fixed-time tracking has been investigated for nonlinear systems with unknown time-varying input delays, improving robustness against delay uncertainties [41]. Furthermore, adaptive fixed-time prescribed performance control has been applied to flexible-joint robotic systems with actuator faults, achieving fast and reliable tracking [42]. Moreover, PPC has demonstrated practical relevance in energy systems. For instance, a distributed power allocation scheme with prescribed performance and intermittent dynamics has been developed for battery energy storage systems under discharge rate constraints in microgrids, where PPC is employed to achieve state-of-charge balancing while satisfying operational limits [43].

Actuator faults pose a serious challenge to the stability and performance of nonlinear control systems. In practical applications, actuators are susceptible to degradation due to aging, wear, and environmental effects, which may result in partial or complete loss of effectiveness. If not properly addressed, such faults can significantly deteriorate tracking performance and may even lead to system instability [44]. Therefore, the development of fault-tolerant control (FTC) strategies capable of compensating for actuator faults is essential to ensure system reliability and safety. Recent research has made notable progress in this direction [45,46]. For example, adaptive fixed-time control schemes have been proposed for nonlinear systems with time-varying actuator faults, achieving rapid fault compensation and maintaining stability [47]. For high-order nonlinear systems with both sensor and actuator faults, adaptive fuzzy fixed-time control approaches have been developed to ensure robust performance within a fixed convergence time [48]. In addition, event-triggered adaptive fixed-time fuzzy control has been introduced for uncertain nonlinear systems with unknown actuator faults, improving efficiency while preserving stability [49]. Furthermore, event-triggered-based fixed-time adaptive fault-tolerant control has been investigated for stochastic nonlinear systems subject to actuator and sensor faults, providing reliable performance under stochastic uncertainties [50]. Despite these advancements, the joint consideration of actuator faults, unknown control coefficients, and prescribed performance within a unified fixed-time control framework remains insufficiently addressed.

The design of effective controllers for nonlinear systems with uncertainties, such as unknown control coefficients, nonlinearities, and actuator faults, remains a challenging problem in control theory. These issues commonly arise in practical engineering systems, for example, in robotic manipulators where actuator degradation, parameter uncertainties, and external disturbances affect system performance. In particular, a single-link manipulator system exhibits nonlinear dynamics and is sensitive to actuator faults and input constraints, making accurate and reliable tracking control a nontrivial task. Fixed-time control methods provide the advantage of guaranteeing convergence within a predefined time, independent of initial conditions. However, incorporating fixed-time control in the

presence of such practical uncertainties is still challenging. Although adaptive control strategies, including command-filter-based approaches, have been developed to address complexity issues, a unified framework that simultaneously ensures prescribed performance, fixed-time convergence, and robustness against uncertainties and actuator faults is still lacking. Motivated by these challenges, this paper investigates the adaptive prescribed performance fixed-time control problem for nonlinear systems and employs command filters to improve implementation efficiency and control performance. The main contributions of this work are summarized as follows:

(i) In contrast to existing work [21,24,28], this paper presents the first approach to address the adaptive prescribed performance fixed-time control problem for uncertain strict-feedback nonlinear systems with unknown control coefficients and actuator faults. A switching control mechanism is proposed to handle the challenge of unknown control coefficients, incorporating a dual-parameter switching strategy with online parameter tuning based on the design conditions. The paper introduces a fixed-time prescribed performance function, ensuring that the system tracking error remains within the defined performance boundary. By simply adjusting the parameters, this function allows for the enforcement of different performance constraints.

(ii) To alleviate the computational burden associated with high-order derivatives in traditional backstepping methods, a command-filter-based backstepping approach is developed. The proposed adaptive controller ensures that all signals in the closed-loop system remain bounded, and the tracking error converges to a small neighborhood of zero within a fixed time. Moreover, the convergence time is independent of the system's initial conditions.

The structure of the paper is organized as follows: Section 2 introduces the problem formulation and provides some preliminary results. The design of the controller, along with its stability analysis, is discussed in Section 3. Section 4 presents simulation examples to validate the proposed method. Finally, Section 5 concludes the paper.

2. Problem Formulation and Preliminaries

Consider the following strict-feedback nonlinear system as

$$\begin{cases} \dot{x}_i = g_i(\bar{x}_i)\, x_{i+1} + \theta_i^T \varphi_i(\bar{x}_i), \quad i = 1, 2, \ldots, n-1, \\ \dot{x}_n = g_n(\bar{x}_n)\, u + \theta_n^T \varphi_n(\bar{x}_n), \\ y = x_1, \end{cases} \tag{1}$$

Consider a nonlinear system where the state vector is defined as $x_i \in [x_1, x_2, \ldots, x_i]^\top \in \mathbb{R}^i$, the system input is $u \in \mathbb{R}$, and the system output is given by $y \in \mathbb{R}$. The system includes unknown parameters $\theta_i \in \mathbb{R}^r$ and nonlinear functions $g_i(\cdot)$, whose signs are also unknown. Additionally, $\phi_i(\cdot) : \mathbb{R}^i \to \mathbb{R}^r$ represent known nonlinear basis functions. The tracking error is expressed as $e(t) = y(t) - y_r(t)$, where $y_r(t)$ denotes a reference trajectory to be tracked. Furthermore, the dynamics of the actuator, which may experience faults, are represented as [50]

$$u(t) = \varpi(t)v(t) + \bar{u}(t) \tag{2}$$

where $\varpi(t)$ is an unknown time-varying function that satisfies $0 < \varpi_{\min} < \varpi(t) \leq 1$, indicating the degree of degradation in the actuator's performance. The signal $v(t)$ is the control input that needs to be designed, while $\bar{u}(t)$ is an unknown fault term that models unexpected actuator malfunctions or abnormal behaviors.

To ensure that the tracking error satisfies the requirements of fixed-time prescribed performance, the following constraint is imposed

$$\mathcal{F}(-\underline{\epsilon}\,\phi(t)) < e(t) < \mathcal{F}(\bar{\epsilon}\,\phi(t)) \tag{3}$$

where $\mathcal{F}(t)$ represents a prescribed performance function, which will be defined later, and the constants $\underline{\epsilon}, \bar{\epsilon} \in (0, 1]$ are design parameters that control the allowable bounds on the tracking error over time.

Prescribed performance function: To achieve fixed-time control objectives for the system, we define the following fixed-time function as

$$r(t) = \begin{cases} \left(\frac{T_c - t}{T_c}\right)^2, & 0 \le t < T_c, \\ 0, & t \ge T_c, \end{cases} \tag{4}$$

where $T_c > 0$ represents the predetermined fixed settling time.T_c is a positive constant representing the prescribed settling time. It is evident that $r(t)$ is continuously differentiable. Next, the performance function is defined as

$$\mathcal{F}(\phi) = \frac{l\phi}{\sqrt{1-\phi^2}} \tag{5}$$

where l is a positive scaling parameter and ϕ is the variable input to the function. The function $\phi(t)$ is defined as a time-dependent scaling function $\phi(t) = (r_0 - r_c)r(t) + r_c$, where the parameters satisfy $0 < r_c < r_0 \le 1$.

Remark 1. *By differentiating $\phi(t)$, we obtain $\dot{\phi}(t) = -\frac{2(r_0 - r_c)}{T_c}\left(1 - \frac{t}{T_c}\right)$, $0 \le t < T_c$, and $\lim_{t \to T_c} \dot{\phi}(t) = 0$. Hence, $\phi(t)$ is a monotonically decreasing function with continuous derivatives. Based on expressions (3)–(5), it follows that the convergence bounds of the tracking error can be adjusted by tuning the parameters $\underline{\epsilon}$, $\bar{\epsilon}$, r_c, and T_c.*

Control objective: For the class of nonlinear systems described by (1), the goal is to develop a fixed-time tracking control scheme that guarantees the tracking error remains strictly within the prescribed convergence bounds given in (2). Furthermore, the design should ensure that all signals within the closed-loop system remain bounded throughout the operation.

To achieve the control objective for system (1), the following assumptions are made.

Assumption 1 ([51]). *The reference tracking signal $y_r(t)$ and its first derivative $\dot{y}_r(t)$ are both known and bounded.*

Assumption 2 ([51]). *The signs of the functions $g_i(\bar{x}_i)$ are unknown, but there exist unknown positive constants $\underline{g_i}$ and $\bar{g}_i$ such that $0 < \underline{g_i} < |g_i(\bar{x}_i)| < \bar{g}_i$ for $i = 1, \ldots, n$.*

Assumption 3 ([50]). *The actuator's additive fault term $\bar{u}(t)$ is assumed to be bounded, i.e., there exists a known positive constant u_0 such that $|\bar{u}(t)| \le u_0$.*

Remark 2. *Assumptions 1 and 2 are standard in the analysis of uncertain nonlinear systems and are introduced to ensure the well-posedness of the control design and stability analysis. In particular, Assumption 2 avoids requiring exact prior knowledge of the control coefficients, which are often uncertain in practical systems, and instead allows them to be handled within the adaptive framework. Compared with existing works such as [45], where actuator degradation is typically modeled as a constant, the actuator fault in model (2) is described as an unknown time-varying function.*

This formulation captures gradual performance degradation more realistically and enhances the applicability of the proposed control scheme to practical scenarios.

3. Controller Design and Stability Analysis

In this section, we present an adaptive switching control scheme for the uncertain nonlinear system described in (1). The proposed control strategy includes two key components: (i) an adaptive state feedback controller utilizing a command filter to reduce computational burden and eliminate the need for higher-order differentiation of the virtual controller, and (ii) an online switching mechanism that dynamically updates the switching parameters to compensate for the unknown control coefficients. To guarantee the performance constraints given in (2), we define the following barrier function:

$$\zeta(t) = \frac{\xi(t)}{\left(\underline{\epsilon} + \xi(t)\right)\left(\bar{\epsilon} - \xi(t)\right)} \tag{6}$$

where $\xi(t)$ is an intermediate variable. Additionally, the following transformation functions are introduced:

$$\xi(t) = \frac{\mu(t)}{\phi(t)}, \quad \mu(t) = \frac{e}{\sqrt{e^2 + l^2}}. \tag{7}$$

Now, the adaptive switching controller is developed based on a command filter combined with a backstepping approach. Initially, the following coordinate transformations are defined:

$$\begin{aligned} z_1(t) &= \zeta(t), \\ z_i(t) &= x_i - \bar{\alpha}_{i-1}, \quad i = 2, \ldots, n. \end{aligned} \tag{8}$$

where $\bar{\alpha}_{i-1}$ represents the output of the command filter. The dynamics of the command filter are given by:

$$\begin{cases} \dot{\vartheta}_{i1} = \omega \vartheta_{i2}, \\ \dot{\vartheta}_{i2} = -2\beta\omega\vartheta_{i2} - \omega(\vartheta_{i1} - \alpha_i), \end{cases} \tag{9}$$

where $\omega > 0$, $0 < \beta \leq 1$, and $\bar{\alpha}_i = \vartheta_{i1}$. The signal α_i serves as the input to the system described in (9). The initial conditions are set as $\vartheta_{i1}(0) = \alpha_i(0)$ and $\vartheta_{i2}(0) = 0$. The compensation error is then defined by

$$\chi_i(t) = z_i - l_i, \quad i = 1, \ldots, n. \tag{10}$$

where l_i represent compensating signals introduced to counteract the effects of the filters. These signals are designed as follows:

$$\begin{cases} \dot{l}_1 = -m_1 \bar{h} l_1 + \varkappa_1 \bar{h}(l_2 + \bar{\alpha}_1 - \alpha_1), \\ \dot{l}_i = -m_i l_i + \varkappa_i (l_{i+1} + \bar{\alpha}_i - \alpha_i), \quad i = 2, \ldots, n-1, \\ \dot{l}_n = -m_n l_n, \end{cases} \tag{11}$$

where m_i are positive design parameters, and $\varkappa_i(k)$ represent switching parameters, which will be developed in Section 3. For $i \in \{1, \ldots, n\}$, let $\hat{\theta}_i$ denote the estimate of the unknown parameter θ_i, and define the estimation error as $\tilde{\theta}_i = \theta_i - \hat{\theta}_i$.

Step 1: Taking the time derivative of z_1 defined in (8), we have

$$\dot{z}_1 = g_1 z_2 + g_1 \bar{\alpha}_1 + \theta_1^\top \varphi_1 - \dot{y}_r - d, \tag{12}$$

where $\bar{h} = \frac{(\underline{\varepsilon}\bar{\varepsilon}+\zeta^2)l^2}{(\phi(\underline{\varepsilon}+\zeta)^2(\bar{\varepsilon}-\zeta)^2(e^2+l^2)\sqrt{e^2+l^2})}$ is a function defined within the prescribed performance bounds, and $d = \frac{(\underline{\varepsilon}\bar{\varepsilon}+\zeta^2)\mu\phi}{\phi^2(\underline{\varepsilon}+\zeta)^2(\bar{\varepsilon}-\zeta)^2}$.

Define the Lyapunov function as

$$V_1 = \frac{1}{2}\chi_1^2 + \frac{1}{2\gamma_1}\tilde{\theta}_1^2, \tag{13}$$

where $\gamma_1 > 0$ is a positive design constant.

Taking the time derivative of(13) gives

$$\begin{aligned}\dot{V}_1 \leq{}& \bar{h}g_1\chi_1\chi_2 + \rho(g_1 - \varkappa_1)\bar{h}\chi_1(l_2 + \bar{\alpha}_1 - \alpha_1) + \bar{h}\theta_1\varphi_1\chi_1 \\ &+ m_1\bar{h}(z_1 - \chi_1)\chi_1 - \dot{y}_r\bar{h}\chi_1 - d\chi_1 + \bar{h}g_1\chi_1\alpha_1 - \frac{1}{\gamma_1}\tilde{\theta}_1\dot{\hat{\theta}}_1.\end{aligned} \tag{14}$$

By applying Young's inequality, one has

$$\frac{\sigma_1}{\gamma_1}\tilde{\theta}_1\hat{\theta}_1 \leq \frac{\sigma_1}{2\gamma_1}\theta_1^2 - \frac{\sigma_1}{2\gamma_1}\tilde{\theta}_1^2 \tag{15}$$

$$\bar{h}g_1\chi_1\chi_2 \leq \frac{c_{11}}{4}\bar{g}_1^2\bar{h}^2\chi_1^2 + \frac{1}{c_{11}}\chi_2^2 \tag{16}$$

$$(g_1 - \varkappa_1)\bar{h}\chi_1(l_2 + \bar{\alpha}_1 - \alpha_1) \leq \frac{c_{12}}{4}(\bar{g}_1 + 1)^2\bar{h}^2\chi_1^2 + \frac{1}{c_{12}}(l_2 + \bar{\alpha}_1 - \alpha_1)^2 \tag{17}$$

where σ_1, c_{11}, and c_{12} are positive design parameters. The virtual control input α_1 and the adaptive update law for the parameter estimate $\hat{\theta}_1$ are then defined as follows:

$$\alpha_1 = -\varkappa_1\bar{h}\lambda\left(\chi_1 + \frac{\hat{\theta}_1^2\varphi_1^2\chi_1}{\sqrt{(\hat{\theta}_1^2\varphi_1^2\bar{h}^2\chi_1^2 + \frac{c_{13}^2}{4})}} + \frac{\varsigma_1^2\chi_1}{\sqrt{(\varsigma_1^2\bar{h}^2\chi_1^2 + \frac{c_{13}^2}{4})}}\right) \tag{18}$$

$$\dot{\hat{\theta}}_1 = \gamma_1\bar{h}\varphi_1\chi_1 - \sigma_1\hat{\theta}_1 \tag{19}$$

where $\varsigma_1 = m_1z_1 - \dot{y}_r - \frac{d}{\bar{h}}$, c_{13} is a positive constant, and $\lambda(t_k, k)$ is a strictly increasing function satisfying $\lim_{k\to\infty}\lambda(t_k, k) = \infty$. By substituting (15)–(19) into (14), and defining $a_1 = \min\{2\bar{h}m_1, \sigma_1\}$, and $\Delta_1 = \frac{\sigma_1}{2\gamma_1}\theta_1^2 + \frac{1}{c_{12}}(l_2 + \bar{\alpha}_1 - \alpha_1)^2 + c_{13}$. Inequality (14) can be rewritten as

$$\dot{V}_1 \leq -a_1V_1 + \Delta_1 - (g_1\varkappa_1\lambda - \hat{c}_1)\left(\varrho_1 + \frac{1}{c_{11}}\chi_2^2\right) \tag{20}$$

where $\hat{c}_1 = \max\left\{\frac{(c_{11}+c_{12})(\bar{g}_1+1)^2}{4}, 1\right\}$ is an unknown constant, and $\varrho_1 = \bar{h}^2\chi_1^2 + \frac{\hat{\theta}_1^2\varphi_1^2\bar{h}^2\chi_1^2}{\sqrt{\hat{\theta}_1^2\varphi_1^2\bar{h}^2\chi_1^2 + \frac{c_{13}^2}{4}}} + \frac{\varsigma_1^2\bar{h}^2\chi_1^2}{\sqrt{\varsigma_1^2\bar{h}^2\chi_1^2 + \frac{c_{13}^2}{4}}} \geq 0$.

Step $i = 2, \ldots, n-1$**:** Taking the time derivative of z_i as defined in (8) gives

$$\dot{z}_i = \dot{x}_i - \dot{\bar{\alpha}}_{i-1} = g_iz_{i+1} + g_i\bar{\alpha}_i + \theta_i\varphi_i - \dot{\bar{\alpha}}_{i-1}. \tag{21}$$

Define the Lyapunov function as

$$V_i = \frac{1}{2}\chi_i^2 + \frac{1}{2\gamma_i}\tilde{\theta}_i^2, \tag{22}$$

where $\gamma_i > 0$ is a known constant.

Using (8), (10), (11), and (21), the time derivative of V_i is given by

$$\dot{V}_i \leq \chi_i\left(g_i\chi_{i+1} + (g_i - \varkappa_i)(l_{i+1} + \bar{\alpha}_i - \alpha_i) + \theta_i\varphi_i - \dot{\bar{\alpha}}_{i-1} + m_i l_i + g_i\alpha_i\right) - \frac{1}{\gamma_i}\tilde{\theta}_i\dot{\hat{\theta}}_i. \quad (23)$$

As with the derivations in (15)–(27), we apply Young's inequality to obtain the following inequalities

$$\frac{\sigma_i}{\gamma_i}\tilde{\theta}_i\hat{\theta}_i \leq \frac{\sigma_i}{2\gamma_i}\theta_i^2 - \frac{\sigma_i}{2\gamma_i}\tilde{\theta}_i^2 \quad (24)$$

$$g_i\chi_i\chi_{i+1} \leq \frac{c_{i1}}{4}\bar{g}_i^2\chi_i^2 + \frac{1}{c_{i1}}\chi_{i+1}^2 \quad (25)$$

$$(g_i - \varkappa_i)\chi_i(l_{i+1} + \bar{\alpha}_i - \alpha_i) \leq \frac{c_{i2}}{4}(\bar{g}_i + 1)^2\chi_i^2 + \frac{1}{c_{i2}}(l_{i+1} + \bar{\alpha}_i - \alpha_i)^2 \quad (26)$$

where σ_i, c_{i1}, and c_{i2} are strictly positive design constants. Based on the inequalities previously derived and after basic simplifications, the expression for the virtual control input α_i and the adaptive parameter update law for $\hat{\theta}_i$ can be formulated as follows:

$$\alpha_i = -\varkappa_i\lambda\left(\chi_i + \frac{\hat{\theta}_i^2\varphi_i^2\chi_i}{\sqrt{\hat{\theta}_i^2\varphi_i^2\chi_i^2 + \frac{c_{i3}^2}{4}}} + \frac{\varsigma_i^2\chi_i}{\sqrt{\varsigma_i^2\chi_i^2 + \frac{c_{i3}^2}{4}}}\right) \quad (27)$$

$$\dot{\hat{\theta}}_i = \gamma_i\varphi_i\chi_i - \sigma_i\hat{\theta}_i \quad (28)$$

where $\varsigma_i = m_i z_i - \dot{\bar{\alpha}}_{i-1}$, and $c_{i3} > 0$ is a constant design parameter. Substituting the inequalities and expressions from (24)–(28) into (23), and defining $a_i = \min\{2m_i, \sigma_i\}$, along with $\Delta_i = \frac{\sigma_i}{2\gamma_i}\theta_i^2 + \frac{1}{c_{i2}}(l_{i+1} + \bar{\alpha}_i - \alpha_i)^2 + c_{i3}$, the derivative of the Lyapunov function V_i can be reformulated as

$$\dot{V}_i \leq -a_i V_i + \Delta_i - (g_i\varkappa_i\lambda - \hat{c}_i)\varrho_i + \frac{1}{c_{i1}}\chi_{i+1}^2 \quad (29)$$

where $\hat{c}_i = \max\left\{\frac{(c_{i1}+c_{i2})(\bar{g}_i+1)^2}{4}, 1\right\}$ represents an unknown positive constant and $\varrho_i = \chi_i^2 + \frac{\hat{\theta}_i^2\varphi_i^2\chi_i^2}{\sqrt{\hat{\theta}_i^2\varphi_i^2\chi_i^2 + \frac{c_{i3}^2}{4}}} + \frac{\varsigma_i^2\chi_i^2}{\sqrt{\varsigma_i^2\chi_i^2 + \frac{c_{i3}^2}{4}}} \geq 0$.

Step n: By using (2) and taking the time derivative of z_n as defined in (8) gives

$$\begin{aligned}\dot{z}_n &= \dot{x}_n - \dot{\bar{\alpha}}_{n-1} \\ &= g_n u + \theta_n\varphi_n - \dot{\bar{\alpha}}_{n-1}, \\ &= g_n\varpi(t)v(t) + g_n\bar{u}(t) + \theta_n\varphi_n - \dot{\bar{\alpha}}_{n-1}\end{aligned} \quad (30)$$

Then, the Lyapunov candidate function for the final step is defined as

$$V_n = \frac{1}{2}\chi_n^2 + \frac{1}{2\gamma_n}\tilde{\theta}_n^2 \quad (31)$$

where $\gamma_n > 0$ is a known positive constant.

By differentiating (31), we obtain the following inequality:

$$\dot{V}_n = -m_n\chi_n^2 + \chi_n(g_n\varpi(t)v(t) + g_n\bar{u}(t) + \theta_n\varphi_n + \varsigma_n) - \frac{1}{\gamma_n}\tilde{\theta}_n\dot{\hat{\theta}}_n \quad (32)$$

where $\varsigma_n = m_n z_n - \dot{\bar{\alpha}}_{n-1}$. Finally, the controller v and the adaptive law for $\hat{\theta}_n$ are given, respectively, as:

$$v = -\kappa_n \lambda \left(\frac{\hat{\theta}_n^2 \varphi_n^2 \chi_n}{\sqrt{(\hat{\theta}_n^2 \varphi_n^2 \chi_n^2 + \frac{c_{n3}^2}{4})}} + \frac{\varsigma_n^2 \chi_n}{\sqrt{(\varsigma_n^2 \chi_n^2 + \frac{c_{n3}^2}{4})}} \right) \tag{33}$$

$$\dot{\hat{\theta}}_n = \gamma_n \varphi_n \chi_n - \sigma_n \hat{\theta}_n \tag{34}$$

where σ_n and c_{n3} are positive parameters.

By employing Young's inequality and Assumptions 2 and 3, one has

$$\chi_n g_n \bar{u}(t) \leq \frac{1}{2} \bar{g}_n \chi_n^2 + \frac{1}{2} \bar{g}_n u_0^2. \tag{35}$$

The following inequality can be concluded:

$$\frac{\sigma_n}{\gamma_n} \tilde{\theta}_n \hat{\theta}_n \leq \frac{\sigma_n}{2\gamma_n} \theta_n^2 - \frac{\sigma_n}{2\gamma_n} \tilde{\theta}_n^2 \tag{36}$$

Then, by defining $a_n = \min\{2m_n, \sigma_n\}$ and $\Delta_n = \frac{\sigma_n}{2\gamma_n} \theta_n^2 + c_{n3} + \frac{1}{2} \bar{g}_n u_0^2$ and by using (33)–(36), inequality (32) can be rewritten as

$$\dot{V}_n \leq -a_n V_n + \Delta_n - \left(g_n \varkappa_n \lambda - 1 \right) \varrho_n, \tag{37}$$

where $\varrho_n = \frac{\hat{\theta}_n^2 \varphi_n^2 \chi_n^2}{\sqrt{\hat{\theta}_n^2 \varphi_n^2 \chi_n^2 + \frac{c_{n3}^2}{4}}} + \frac{\varsigma_n^2 \chi_n^2}{\sqrt{\varsigma_n^2 \chi_n^2 + \frac{c_{n3}^2}{4}}} \geq 0$.

It is important to note that $\varrho_i \geq 0$ for all $i = 1, \ldots, n$. Therefore, the primary task is to design the function $\lambda(t_k, k)$ such that $\lambda(t_k, k) - \max\left\{ \frac{\hat{c}_i}{|g_i|}, \frac{1}{|g_n|} \right\} \geq 0$, and, by employing the switching mechanism, ensure that $\varkappa_i = \text{sign}(g_i)$ is achieved within a finite number of switches.

Now, a switching mechanism is introduced to adaptively update the parameters t_k and k. To begin with, we define the following function as

$$W(t_k, t) = \max\{\rho(t_k, t), \hat{V}(t)\} \tag{38}$$

where $\rho(t_k, t)$ and $\hat{V}(t)$ represent the monitoring function and the Lyapunov-like function, respectively. These are defined as follows:

$$\rho(t_k, t) = \left(W(t_k) - \rho_\infty(t_k) \right) e^{-\epsilon_1 (t - t_k)} + \rho_\infty(t_k) \tag{39}$$

$$V(t) = \sum_{i=1}^{n} \left(\frac{1}{2} \chi_i^2 + \frac{1}{2\gamma_i} \hat{\theta}_i^2 \right) \tag{40}$$

where ϵ_1 is a design parameter. Next, the candidate symbolic function $\kappa(k)$ is defined as:

$$\varkappa(k) = \begin{cases} N(0), & k = K \cdot 2^n \\ N(1), & k = K \cdot 2^n + 1 \\ \vdots & \\ N(2^n - 1), & k = K \cdot 2^n + 2^n - 1 \end{cases} \tag{41}$$

where $K := \left\lfloor \frac{k}{2^n} \right\rfloor$ and $N(j) = [\varkappa_1, \ldots, \varkappa_n], \quad \varkappa_i = \pm 1, \quad i = 1, \ldots, n, \quad j = 0, \ldots, 2^n - 1$. The switching rule $k(t)$ is formulated as

$$k(t) = \begin{cases} \kappa, & \text{if } \hat{V} \leq \rho(t_k, t), \quad t \geq t_k \\ \kappa + 1, & \text{otherwise.} \end{cases} \tag{42}$$

Theorem 1. *For the system (1) with unknown control coefficients and actuator faults (2), the system tracking error satisfies the fixed-time prescribed performance requirements (3) by designing the controller (33) and the switching mechanisms (38)–(42). Moreover, all closed-loop signals are bounded.*

Proof. The proof is organized in two cases. The first case shows that the control objective of Theorem 1 can be fully realized after the controller switches a finite number of times. The second case proves that the switching mechanism will not be triggered indefinitely.

Case 1: First, denote $\bar{k}$ as the index of the last switching occurrence, and let the corresponding time be $t_{\bar{k}}$. For $t \geq t_{\bar{k}}$, based on the results in [52], the inaccuracy of $|\bar{\alpha}_i - \alpha_i|$ is unknown but bounded. Thus, the compensation signals l_i are bounded. By designing $a = \min_{1\leq i\leq n}\left\{a_i - \frac{2}{c_{i1}}\right\}$, it follows that

$$\dot{V} \leq -aV + \Delta. \tag{43}$$

where $V = \sum_{i=1}^{n} V_i$ and $\Delta = \sum_{i=1}^{n} \Delta_i$. Thus, we conclude that l_i and $\tilde{\Xi}$ are bounded, and consequently V_i, χ_i, z_i, and x_i are bounded. All signals in $\hat{\dot{\theta}}_i$, α_i, and u are bounded. Finally, we conclude that all closed-loop signals are bounded. This means that ζ is bounded. In summary, the system tracking error meets the specified performance requirements.

Case 2: At this stage, it is proved that the switching mechanism does not experience Zeno's phenomenon employing the method of contradiction. We first assume that switching occurs an infinite number of times. From (20), (29), and (37), it can be derived directly that

$$|\chi_i| \leq \sqrt{2\left(V(0) + \frac{\Delta}{a}\right)} \triangleq \Delta \tag{44}$$

$$|\hat{\theta}_i| \leq \sqrt{2\gamma_i\left(V(0) + \frac{\Delta}{a}\right)} + |\theta_i| \triangleq \Gamma \tag{45}$$

$$|\hat{\dot{\theta}}_i| \leq \gamma\varphi\Lambda + \sigma\Gamma \triangleq \Xi \tag{46}$$

where $\bar{\varphi}$ is the upper bound of φ_i. Then, the following inequality can be derived:

$$\begin{aligned}
\dot{\hat{V}} &\leq -aV + \Delta + \sum_{i=1}^{n} \frac{1}{\gamma_i}\theta_i\hat{\dot{\theta}}_i \\
&\leq -a\hat{V} + \Delta + \sum_{i=1}^{n} \frac{1}{\gamma_i}\theta_i\hat{\dot{\theta}}_i + \sum_{i=1}^{n} \frac{a}{\gamma_i}\theta_i\hat{\theta}_i - \sum_{i=1}^{n} \frac{a}{2\gamma_i}\theta_i^2 \\
&\leq -a\hat{V} + \hat{\Delta}
\end{aligned} \tag{47}$$

where $\hat{\Delta} = \Delta + \sum_{i=1}^{n} \frac{1}{\gamma_i}\theta_i\Xi + \sum_{i=1}^{n} \frac{a}{\gamma_i}\theta_i\Gamma$ is a positive constant. Suppose there exists a switching trigger moment $t_{\bar{k}+1}$, such that $\hat{V} \leq \frac{\hat{\Delta}}{a}$, on $[t_s, t_{\bar{k}+1})$, where t_s is the first time instant satisfying $\hat{V} = \frac{\hat{\Delta}}{a}$. Then, $\dot{\hat{V}} \leq 0$ holds when $\hat{V} \geq \frac{\hat{\Delta}}{a}$. For $t > t_{\bar{k}}$, $\hat{V}$ strictly decreases on $[t_{\bar{k}}, t_s)$, implying that no new switching occurs on $[t_{\bar{k}}, t_s)$ and $t_s < t_{\bar{k}+1}$. The steady-state value of the monitoring function is selected such that $\rho_\infty(t_k) \geq \frac{\hat{\Delta}}{a} + \epsilon_2$, where $\epsilon_2 > 0$ is a small design constant. Since $\hat{\Delta}$ is a positive constant and $a > 0$ is determined by controller design, this condition can always be satisfied by appropriate selection of $\rho_\infty(t_k)$. Under this condition, once $\hat{V}(t)$ enters the compact set $\hat{V}(t) \leq \frac{\hat{\Delta}}{a}$, the inequality $\hat{V}(t) \leq \rho(t_k, t)$ holds, and the switching condition is no longer triggered, thereby excluding Zeno behavior. When $t \in [t_s, t_{\bar{k}+1})$, the condition $\rho_\infty(t_k) \geq \frac{\hat{\Delta}}{a}$ can be satisfied. Consequently, $\hat{V} \leq \rho$ holds on $t \in [t_s, t_{\bar{k}+1})$. In summary, we have $\hat{V} \leq \rho(t_k, t) + \epsilon_2$ on $[t_{\bar{k}}, t_{\bar{k}+1})$, which implies that the switching condition (42) is never fulfilled. This completes the proof. □

Remark 3. *It is important to note that the terms* $(g_i\varkappa_i\lambda - \hat{c}_i)\varrho_i$ *appearing in (20), (29), and (37) satisfy the required non-negativity condition under the proposed switching mechanism. Specifically, the switching law systematically generates all possible combinations of* $\varkappa_i \in \{+1, -1\}$*, and thus there exists a finite switching index such that* $\varkappa_i = \text{sign}(g_i)$ *for all* $i = 1, \ldots, n$*, yielding* $g_i\varkappa_i = |g_i|$*. Meanwhile, the adaptive parameter* $\lambda(t_k, k)$ *is selected to satisfy* $\lambda(t_k, k) \geq \frac{\hat{c}_i}{|g_i|}$*. Consequently, it follows that* $g_i\varkappa_i\lambda - \hat{c}_i \geq 0$*. Since* $\varrho_i \geq 0$*, the terms in (20), (29), and (37) are ensured to be non-negative, which guarantees the validity of the stability analysis.*

Figure 1 provides an overview of the configuration adopted in the designed control framework.

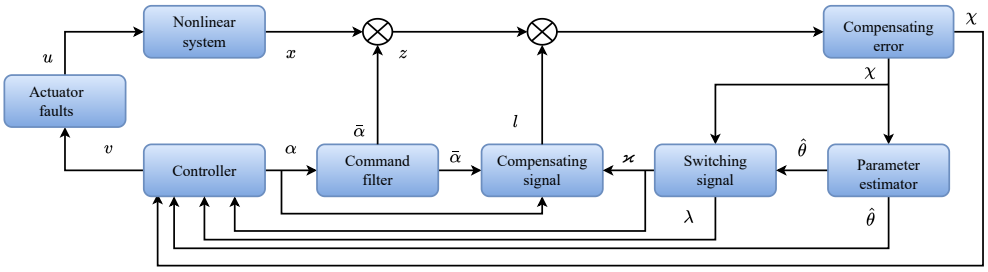

Figure 1. Schematic representation of the proposed control framework architecture.

4. Simulation Examples

To validate the performance and robustness of the proposed control strategy, this section presents two simulation examples.

Example 1. *Consider the following nonlinear systems as*

$$\begin{cases} \dot{x}_1 &= g_1(x_1)x_2 + \varphi_1(x_1), \\ \dot{x}_2 &= g_2(x_2)u + \varphi_2(x_2), \\ y &= x_1, \end{cases} \tag{48}$$

where $\varphi_1(x_1) = 0.1x_1^2$*,* $\varphi_2(x_2) = x_1x_2^2$*,* $g_1(x_1) = 2sign(g_1)(2 - 0.4\sin(x_1))$*,* $g_2(x_2) = sign(g_2)(4 - 0.1e^{x_1x_2})$*. The desired trajectory to be followed by the system output is specified as* $y_r(t) = \sin(t)$*. The actuator failure model can be described as*

$$u(t) = \begin{cases} v(t), & t < 10, \\ (0.6 + 0.3\sin(t))v(t) + \bar{u}(t), & t \geq 10, \end{cases} \tag{49}$$

where the fault signal is defined by $\bar{u}(t) = 2\cos(0.5t)$*. The parametric uncertainties associated with the system are given by the vector* $\theta = [1 \;\; 1]^T$*. The initial estimates for the unknown parameters are chosen as* $\hat{\theta}(0) = [0.2 \;\; 0.2]^T$*, and the adaptive gains are initialized with* $l(0) = [0.5 \;\; 0.5]^T$*. The initial condition for the system state is selected as* $[x_1(0) \;\; x_2(0)]^T = [0.5 \;\; 0.5]^T$*. The control design parameters are set as follows:* $T_c = 0.5$*,* $r_c = 0.2$*,* $\gamma_1 = 0.6, \gamma_2 = 0.8$*,* $\sigma_1 = \sigma_2 = 1$*, and* $m_1 = m_2 = 3$*. The initial tracking error is given by* $e(0) = 0.3$*. The simulation results are illustrated in Figures 2–6. As evident from Figure 2, the system output* y *accurately tracks the reference signal* y_r*, demonstrating the proposed control method's strong performance in trajectory tracking. The progression of the tracking error* $e(t)$ *is shown in Figure 3, where the error decreases toward zero, confirming the controller's precision and compliance with the prescribed constraint* $\mathcal{F}(-\underline{\epsilon}\,\phi(t)) < e(t) < \mathcal{F}(\bar{\epsilon}\,\phi(t))$*. An actuator fault is introduced at* $t \geq 10$*, and its effects are clearly visible in the highlighted segments of Figures 3, 4, and 6. Specifically, Figure 3 captures a temporary fluctuation in the tracking error following fault activation, reflecting the system's*

sensitivity to the actuator degradation. Figure 4 portrays the dynamics of the state variable x_2, where the impact of the fault appears as a noticeable alteration in its trajectory. Figure 5 illustrates the behavior of the adaptive parameters $\hat{\theta}_1$ and $\hat{\theta}_2$, confirming that these parameters remain bounded and adapt smoothly in the presence of faults. Figure 6 compares the designed control signal v and the actual control input u, highlighting the actuator fault's influence and the controller's ability to counteract its effects and maintain system stability. Collectively, these simulation figures validate that the developed adaptive control scheme ensures fixed-time convergence and preserves the boundedness of all signals in the closed-loop system.

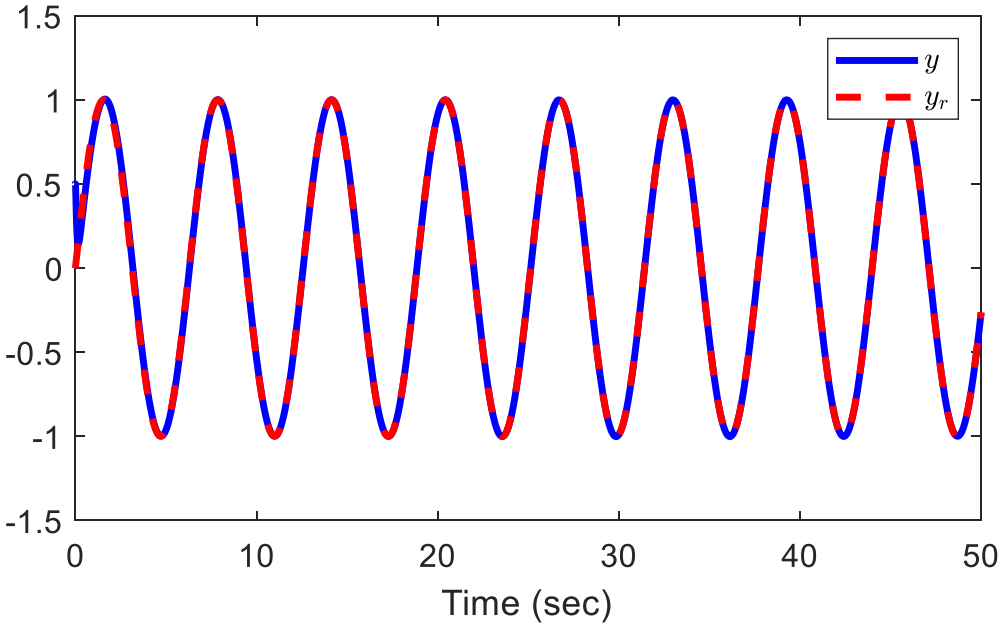

Figure 2. Trajectories of the system output y and the reference signal y_d.

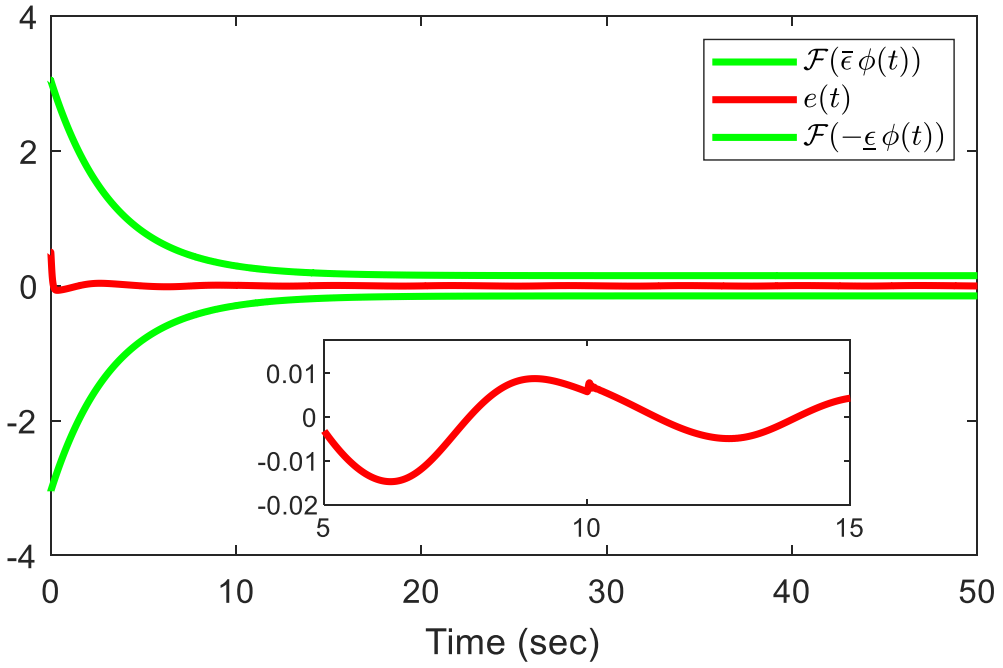

Figure 3. Trajectory of the tracking error $e(t)$.

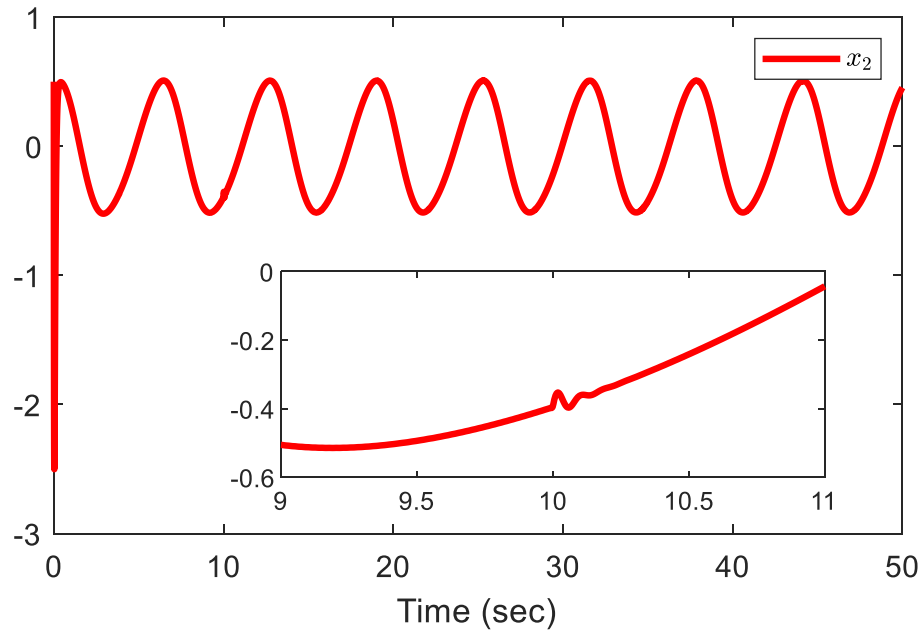

Figure 4. System state x_2.

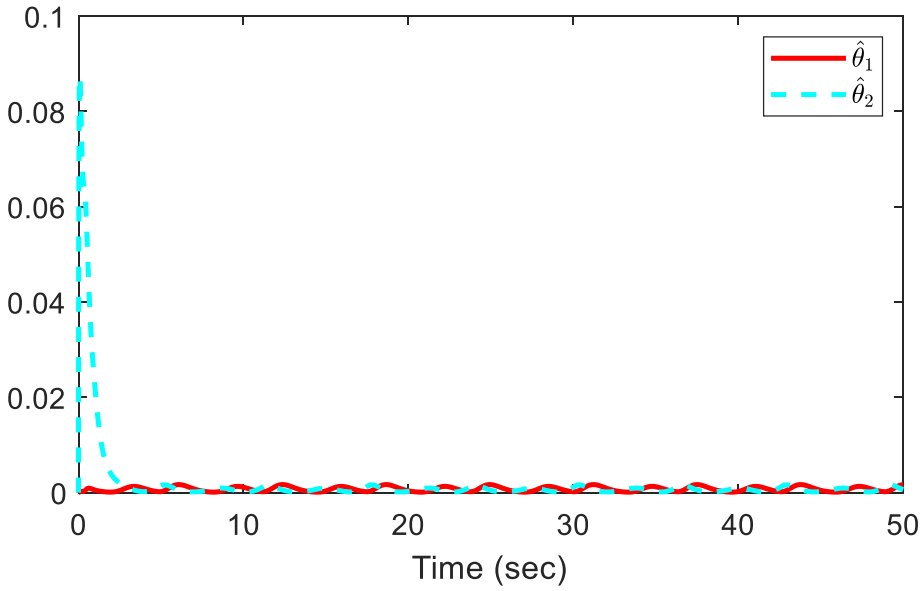

Figure 5. Adaptive parameters $\hat{\theta}_1$ and $\hat{\theta}_2$.

Comparative Performance Analysis: *To demonstrate the effectiveness of the proposed adaptive control framework, a comparative study is conducted against the method presented in [26], which considers adaptive finite-time control for stochastic nonlinear systems with input saturation based on a multidimensional Taylor network. This method is selected as a benchmark due to its capability to handle nonlinear dynamics and input constraints, making it suitable for a meaningful comparison with the proposed approach. Both controllers are implemented under identical simulation conditions to ensure a fair and consistent evaluation. The tracking performance is assessed using standard error metrics computed from the system output $y(t)$ and the reference signal $y_r(t)$ over N sampling instants. The employed performance indices are defined as follows:*

Maximum Absolute Error (MAE):

$$MAE = \max_{1 \le t \le N} |y(t) - y_r(t)|. \tag{50}$$

Sum of Squared Errors (SSE):

$$SSE = \sum_{t=1}^{N} (y(t) - y_r(t))^2. \tag{51}$$

Mean Squared Error (MSE):

$$MSE = \frac{1}{N} \sum_{t=1}^{N} (y(t) - y_r(t))^2. \tag{52}$$

Root Mean Squared Error (RMSE):

$$RMSE = \sqrt{\frac{1}{N} \sum_{t=1}^{N} (y(t) - y_r(t))^2}. \tag{53}$$

Normalized Mean Squared Error (NMSE):

$$NMSE = \frac{\sum_{t=1}^{N} (y(t) - y_r(t))^2}{\sum_{t=1}^{N} (y_r(t) - \bar{y}_r)^2}. \tag{54}$$

Best Fit Rate (BFR):

$$BFR = \left(1 - \frac{\sqrt{\sum_{t=1}^{N} (y(t) - y_r(t))^2}}{\sum_{t=1}^{N} |y_r(t) - \bar{y}_r|} \right) \times 100\%. \tag{55}$$

As observed from Table 1, the proposed scheme achieves distinctly improved performance across all indicators. The considerable reductions in MAE, SSE, MSE, RMSE, and NMSE highlight more precise tracking behavior and smaller deviations from the reference trajectory. Furthermore, the noticeably higher BFR signifies stronger alignment and consistency with $y_r(t)$. Overall, the results verify the effectiveness, robustness, and superior tracking capability of the proposed control approach in uncertain nonlinear environments.

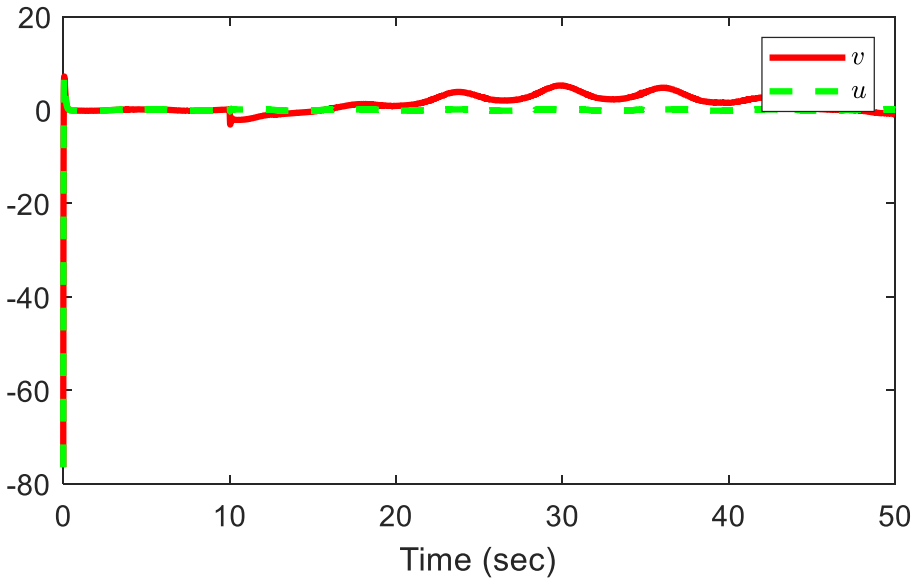

Figure 6. Control signal v and the system input u.

Table 1. Error-index comparison between the proposed control strategy and the method in [26].

Controller	MAE	SSE	MSE	RMSE	NMSE	BFR (%)
Proposed Controller	0.1587	3.7426	0.000412	0.0203	0.00264	99.94
Method in [26]	0.2891	5.9814	0.000660	0.0257	0.00438	99.69

Example 2. *To further evaluate the efficiency of the proposed adaptive control scheme, consider a single-link robotic manipulator system shown in Figure 7 described in [51], which is modeled by the following dynamic equation:*

$$J\ddot{q} + C\dot{q} + Mgl\sin(q) = u, \tag{56}$$

where q and $\dot{q}$ represent the angular position and angular velocity of the rigid link, respectively. The constants J, C, l, M, and g correspond to the moment of inertia, damping coefficient, distance from the joint axis to the link's center of mass, mass of the link, and gravitational acceleration, respectively.

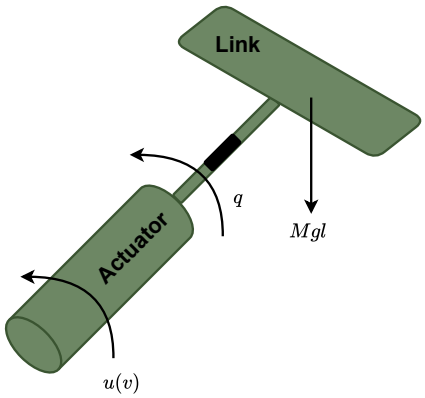

Figure 7. A single-link robot manipulator.

The physical parameters are assigned as $J = 1$, $Mgl = 10$, and $C = 2$. By defining the state variables as $x_1 = q$ and $x_2 = \dot{q}$, the system dynamics can be rewritten in state-space form:

$$\begin{cases} \dot{x}_1 &= x_2, \\ \dot{x}_2 &= \varphi_2(x_1, x_2) + g_2(x_2)u, \\ y &= x_1, \end{cases} \tag{57}$$

where the nonlinear functions are given by $\varphi_2(x_1, x_2) = -\frac{C}{J}x_2 - \frac{MgL}{J}\sin(x_1)$, $g_1(x_1) = 1$, $g_2(x_2) = sign(g_2)(\frac{1}{J})$. The desired trajectory to be tracked is set as $y_d = 0.5\sin(t)$. In this example, the control gain is taken as $g_2(x_2) = \frac{\text{sign}(g_2)}{J} = \pm 1$, representing a known magnitude with unknown control direction. The actuator failure model can be described as

$$u(t) = \begin{cases} v(t), & t < 10, \\ (0.6 + 0.3\sin(t))v(t) + \bar{u}(t), & t \geq 10, \end{cases} \tag{58}$$

where the fault signal is defined by $\bar{u}(t) = 2\cos(0.5t)$. The parametric uncertainties associated with the system are given by the vector $\theta = [1 \;\; 1]^T$. The initial estimates for the unknown parameters are chosen as $\hat{\theta}(0) = [0.2 \;\; 0.2]^T$, and the adaptive gains are initialized with $l(0) = [0.5 \;\; 0.5]^T$. The initial condition for the system state is selected as $[x_1(0) \;\; x_2(0)]^T = [0.5 \;\; 0.5]^T$. The control design parameters are set as follows: $T_c = 0.5$, $r_c = 0.2$, $\gamma_1 = \gamma_2 = 0.1$, $\sigma_1 = \sigma_2 = 4$, and $m_1 = m_2 = 5$. The initial tracking error is given by $e(0) = 0.3$. The simulation outcomes corresponding to Example 2 are presented in Figures 8–12. As depicted in Figure 8, the system output y closely

follows the desired reference trajectory y_r, illustrating the effectiveness of the proposed control framework in achieving accurate tracking performance. Figure 9 displays the evolution of the tracking error $e(t)$, which converges toward zero, satisfying the prescribed performance bounds $\mathcal{F}(-\underline{\epsilon}\,\phi(t)) < e(t) < \mathcal{F}(\bar{\epsilon}\,\phi(t))$. At time $t \geq 10$, an actuator fault is introduced into the system. The immediate impact of this fault is evident in the zoomed-in portions of Figures 9, 10, and 12. Notably, Figure 9 shows a transient deviation in the tracking error following the fault occurrence, indicating the system's response to actuator degradation. Figure 10 highlights the behavior of the internal state x_2, where a change in trajectory clearly signals the onset of the fault. Figure 11 shows the trajectories of the adaptive estimates $\hat{\theta}_1$ and $\hat{\theta}_2$, which remain bounded and exhibit stable adaptation even after the fault is introduced. In Figure 12, the designed virtual control input v is plotted alongside the actual applied input u, clearly revealing the mismatch caused by the actuator fault and the control system's successful compensation strategy. These simulation plots collectively confirm that the proposed controller maintains closed-loop stability, enforces the desired tracking performance, and ensures fixed-time convergence despite the presence of actuator faults.

Performance Evaluation for Example 2: *To further demonstrate the effectiveness and robustness of the proposed control framework, a second numerical example is considered and compared with the method reported in [26]. The selected reference method addresses adaptive finite-time control for stochastic nonlinear systems with input saturation, making it a relevant benchmark for comparison. Both controllers are evaluated under identical simulation conditions to ensure a fair assessment. The tracking performance is quantified using standard error indices computed from the system output $y(t)$ and the reference signal $y_r(t)$. The comparative results are summarized in Table 2, which clearly illustrate the improved tracking accuracy and convergence characteristics of the proposed approach.*

From Table 2, it is evident that the proposed controller delivers improved performance across all evaluated metrics. The lower MAE, SSE, MSE, RMSE, and NMSE values indicate more accurate tracking and reduced deviation from the desired trajectory. In addition, the higher BFR value confirms that the proposed approach achieves a closer match with the reference signal $y_r(t)$, demonstrating stronger robustness and enhanced control quality for Example 2.

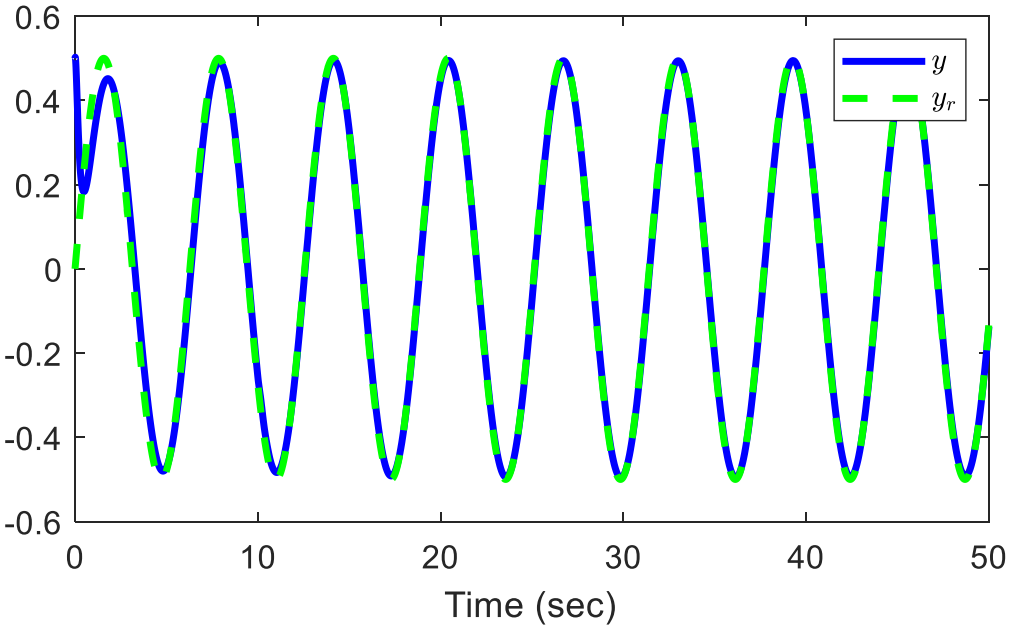

Figure 8. Trajectories of the system output y and the reference signal y_r.

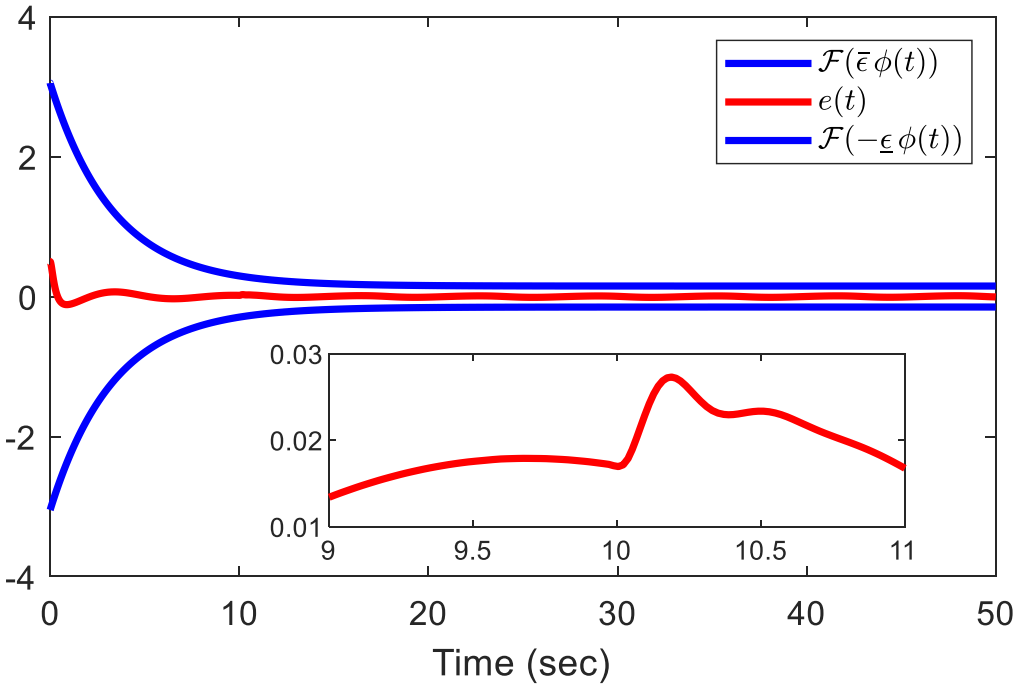

Figure 9. Trajectory of the tracking error z_1.

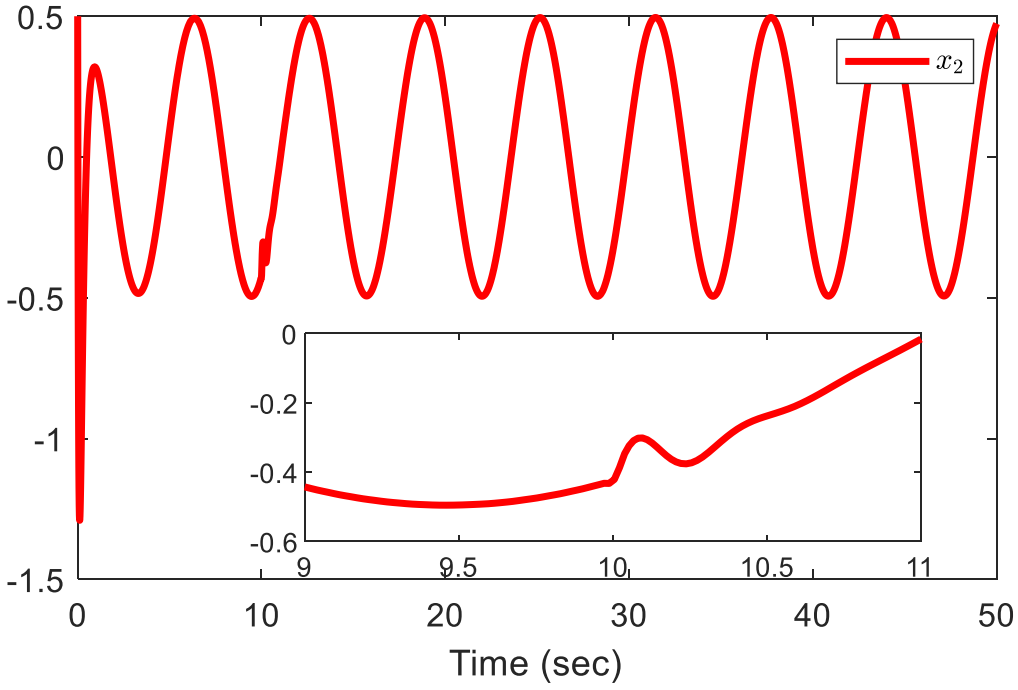

Figure 10. System state x_2.

Table 2. Tracking performance comparison for Example 2 between the proposed control scheme and the method in [26].

Controller	MAE	SSE	MSE	RMSE	NMSE	BFR (%)
Proposed Controller	0.1294	2.6815	0.000291	0.0171	0.00183	99.97
Method in [26]	0.2457	4.9132	0.000552	0.0235	0.00366	99.74

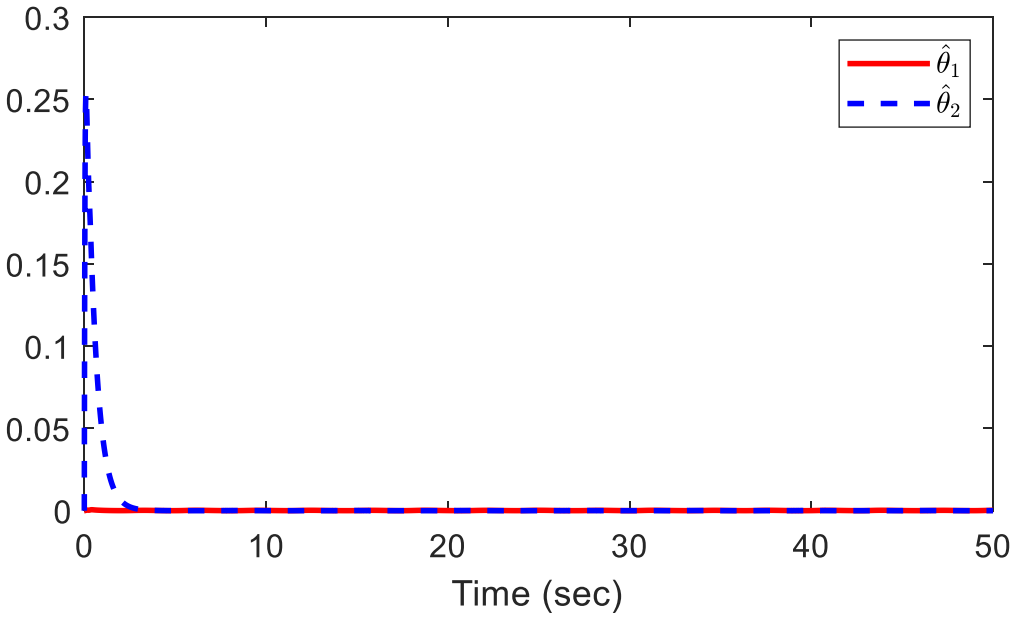

Figure 11. Adaptive parameters $\hat{\theta}_1$ and $\hat{\theta}_2$.

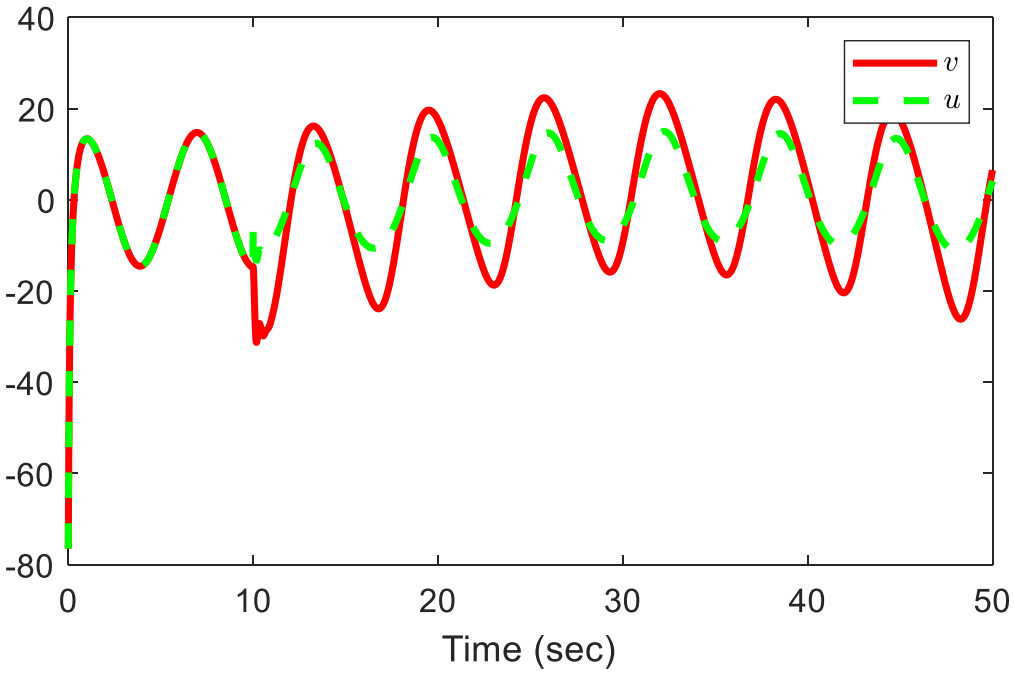

Figure 12. Control signal v and the system input u.

Remark 4. *It is worth noting that the considered nonlinear systems are subject to uncertainties, unknown control coefficients, and actuator faults. In the absence of the proposed control strategy, these factors may lead to significant tracking errors or even instability. The satisfactory tracking performance observed in the simulation results is achieved due to the designed controller, which actively compensates for these uncertainties and ensures fixed-time convergence.*

Remark 5. *In the presence of actuator faults, the control input is affected by unknown, time-varying disturbances that may degrade system performance. In the proposed framework, these faults are not directly measured but are incorporated into the system model as uncertainties. The adaptive mechanism continuously adjusts the control parameters online to compensate for their effects. As a result, the influence of actuator faults is effectively mitigated, allowing the system to maintain stable*

behavior and achieve accurate tracking within a fixed time. This explains why the system output is still able to follow the desired reference trajectory despite the occurrence of actuator faults.

Remark 6. *It should be noted that inequality (43), i.e., $\dot{V} \leq -aV + \Delta$, only guarantees boundedness of all closed-loop signals and convergence to a compact set. The fixed-time convergence property of the tracking error is not directly derived from this inequality. Instead, it is ensured by the prescribed performance function defined in (3), which constrains the tracking error within a predefined performance envelope that converges to a small residual set within a fixed time independent of the initial conditions. Through the prescribed performance transformation, the original tracking error is mapped into an unconstrained variable, whose boundedness implies that the tracking error satisfies the fixed-time prescribed performance requirements.*

Remark 7. *The performance of the proposed control scheme depends on the selection of the convergence time T_c and the ultimate bound in the prescribed performance function. The parameter T_c determines the rate at which the performance boundary shrinks, while the ultimate bound specifies the steady-state accuracy. A smaller T_c leads to faster convergence but may require higher control effort, whereas a larger T_c results in slower convergence. Similarly, choosing a smaller ultimate bound improves tracking precision at the expense of increased control activity. Nevertheless, due to the adaptive and robust nature of the proposed design, the closed-loop system remains stable and satisfies the prescribed performance constraints under reasonable variations of these parameters.*

5. Conclusions

This paper tackles the adaptive prescribed performance fixed-time control problem for uncertain strict-feedback nonlinear systems with unknown control coefficients and actuator faults. A switching control mechanism is proposed to address the challenges associated with unknown control coefficients, utilizing a dual-parameter switching strategy with online parameter tuning based on the design conditions. A fixed-time prescribed performance function is introduced to ensure that the system's tracking error remains within the desired performance limits. The issue of "explosion of complexity" is alleviated by employing the command filter method, with errors from the filters being compensated by the introduction of appropriate corrective signals. Lyapunov stability analysis demonstrates that the closed-loop system achieves semiglobal fixed-time stability, with the tracking error converging to a small neighborhood of zero within a fixed time, independent of the system's initial conditions. Finally, both numerical and practical examples are presented to validate the proposed control method's effectiveness and feasibility. In future work, we aim to extend this approach to real-world applications, such as quadrotor systems, by incorporating sensor faults and full-state constraints, based on fixed-time stability theory.

Author Contributions: H.A.: Writing—original draft, Investigation; M.K.: Supervision, Writing—review and editing; A.A.-J.: Validation; P.M.: Supervision, Writing—review and editing. All authors have read and agreed to the published version of the manuscript.

Funding: This research received no external funding.

Data Availability Statement: The original contributions presented in this study are included in the article. Further inquiries can be directed to the corresponding author.

Acknowledgments: The authors extend their appreciation to the Deanship of Scientific Research and Libraries at Princess Nourah bint Abdulrahman University for funding this research work through the Supporting Publication in Top-Impact Journals Initiative (SPTIF-2026).

Conflicts of Interest: The authors declare no conflicts of interest.

References

1. Kharrat, M.; Mercorelli, P. Predefined-time adaptive command filter control for nonstrict-feedback nonlinear systems with input delay and unmodeled dynamics. *Mathematics* **2025**, *14*, 14. [CrossRef]
2. Shi, S.; Dai, B.; Min, H. Adaptive finite-time control for stochastic nonlinear systems with multiple uncertainties. *Int. J. Syst. Sci.* **2025**, *56*, 1–12. [CrossRef]
3. Kharrat, M.; Mercorelli, P. Neural network-based adaptive finite-time control for pure-feedback stochastic nonlinear systems with full state constraints, actuator faults, and backlash-like hysteresis. *Mathematics* **2025**, *14*, 30. [CrossRef]
4. Han, Y.Q.; Zhu, S.L.; Duan, D.Y.; Yang, S.G. Adaptive neural output feedback tracking control for a class of nonlinear systems. *Int. J. Syst. Sci.* **2019**, *50*, 2088–2101. [CrossRef]
5. Kharrat, M.; Krichen, M.; Alhazmi, H.; Mercorelli, P. Neural network-based finite-time control for stochastic nonlinear systems with input dead-zone and saturation. *Arab. J. Sci. Eng.* **2025**, 17369–17379. [CrossRef]
6. Kharrat, M. Adaptive neural dynamic surface control for high-order nonstrict-feedback nonlinear systems with unknown backlash-like hysteresis and actuator faults. *Int. J. Syst. Sci.* **2025**, 1–18. [CrossRef]
7. Xu, N.; Zhao, X.; Zong, G.; Wang, Y. Adaptive control design for uncertain switched nonstrict-feedback nonlinear systems to achieve asymptotic tracking performance. *Appl. Math. Comput.* **2021**, *408*, 126344. [CrossRef]
8. Wang, H.; Xu, K.; Liu, P.X.; Qiao, J. Adaptive fuzzy fast finite-time dynamic surface tracking control for nonlinear systems. *IEEE Trans. Circuits Syst. I* **2021**, *68*, 4337–4348. [CrossRef]
9. Zhai, J.; Wang, H.; Tao, J. Disturbance-observer-based adaptive dynamic surface control for nonlinear systems with input dead-zone and delay using neural networks. *Neural Comput. Appl.* **2023**, *35*, 4027–4049. [CrossRef]
10. Zhang, J.; Pan, Y.; Cao, L. Command filter-based adaptive fault-tolerant tracking control for switched nonlinear systems with time-varying output constraints. *Nonlinear Anal. Hybrid Syst.* **2024**, *52*, 101478. [CrossRef]
11. Chen, M.; Li, Y.; Wang, H.; Peng, K.; Wu, L. Adaptive fixed-time tracking control for nonlinear systems based on finite-time command-filtered backstepping. *IEEE Trans. Fuzzy Syst.* **2023**, *31*, 1604–1613. [CrossRef]
12. Sui, S.; Chen, C.P.; Tong, S. Command filter based predefined-time adaptive control for nonlinear systems. *IEEE Trans. Autom. Control* **2024**, *69*, 7863–7870. [CrossRef]
13. Yang, Y.; Tang, L.; Zou, W.; Ding, D.W. Robust adaptive control of uncertain nonlinear systems with unmodeled dynamics using command filter. *Int. J. Robust Nonlinear Control* **2021**, *31*, 7764–7784. [CrossRef]
14. Ding, J.; Zhang, W. Finite-time adaptive control for nonlinear systems with uncertain parameters based on the command filters. *Int. J. Adapt. Control Signal Process.* **2021**, *35*, 1754–1767. [CrossRef]
15. Wang, H.; Kang, S.; Zhao, X.; Xu, N.; Li, T. Command filter-based adaptive neural control design for nonstrict-feedback nonlinear systems with multiple actuator constraints. *IEEE Trans. Cybern.* **2021**, *52*, 12561–12570. [CrossRef] [PubMed]
16. Kang, S.; Liu, P.X.; Wang, H. Command filter-based adaptive fuzzy decentralized control for large-scale nonlinear systems. *Nonlinear Dyn.* **2021**, *105*, 3239–3253. [CrossRef]
17. Chen, Z.; Niu, B.; Zhang, L.; Zhao, J.; Ahmad, A.M.; Alassafi, M.O. Command filtering-based adaptive neural network control for uncertain switched nonlinear systems using event-triggered communication. *Int. J. Robust Nonlinear Control* **2022**, *32*, 6507–6522. [CrossRef]
18. Deng, X.; Zhang, C.; Ge, Y. Adaptive neural network dynamic surface control of uncertain strict-feedback nonlinear systems with unknown control direction and unknown actuator fault. *J. Frankl. Inst.* **2022**, *359*, 4054–4073. [CrossRef]
19. Zhang, J.; Xiang, Z. Event-triggered adaptive neural network sensor failure compensation for switched interconnected nonlinear systems with unknown control coefficients. *IEEE Trans. Neural Netw. Learn. Syst.* **2021**, *33*, 5241–5252. [CrossRef]
20. Wu, J.; Sun, W.; Su, S.F.; Wu, Y. Adaptive asymptotic tracking control for input-quantized nonlinear systems with multiple unknown control directions. *IEEE Trans. Cybern.* **2022**, *53*, 5216–5225. [CrossRef]
21. Guo, J.; Bo, Y.; Park, J.H.; Ma, J. Adaptive neural control for nonlinear systems with actuator faults and unknown control directions via command filter. *Int. J. Robust Nonlinear Control* **2022**, *32*, 2100–2118. [CrossRef]
22. Liu, C.; Liu, X.; Wang, H.; Lu, S.; Zhou, Y. Adaptive control and application for nonlinear systems with input nonlinearities and unknown virtual control coefficients. *IEEE Trans. Cybern.* **2021**, *52*, 8804–8817. [CrossRef] [PubMed]
23. Ju, X.; Jia, X.; Shi, X.; Yu, S.E. Adaptive output feedback event-triggered tracking control for nonlinear systems with unknown control coefficient. *Appl. Math. Comput.* **2022**, *432*, 127369. [CrossRef]
24. Liu, C.; Gao, C.; Liu, X.; Wang, H.; Zhou, Y. Adaptive finite-time prescribed performance control for stochastic nonlinear systems with unknown virtual control coefficients. *Nonlinear Dyn.* **2021**, *104*, 3655–3670. [CrossRef]
25. Zhao, W.; Han, Y.Q.; Zhou, Y.F.; Zhu, S.L. Adaptive finite-time tracking control of nonlinear systems subject to input hysteresis and multiple objective constraints. *Int. J. Robust Nonlinear Control* **2024**, *34*, 10292–10314. [CrossRef]

26. Han, Y.Q.; Sun, J.J. Adaptive finite-time control for a class of stochastic nonlinear systems with input saturation constraints: A new approach based on multidimensional Taylor network. *Int. J. Robust Nonlinear Control* **2024**, *34*, 5329–5345. [CrossRef]
27. Jin, Y.; Wang, F.; Zhao, M. Predefined-time adaptive fuzzy tracking control for switched nonlinear systems. *Asian J. Control* **2024**, *26*, 1927–1938. [CrossRef]
28. Ma, J.; Wang, H.; Qiao, J. Adaptive neural fixed-time tracking control for high-order nonlinear systems. *IEEE Trans. Neural Netw. Learn. Syst.* **2022**, *35*, 708–717. [CrossRef]
29. Zhang, C.H.; Li, Y.J.; Hua, C.C.; Zhang, Y. A new event-triggered adaptive fixed-time control design for uncertain nonlinear systems. *IEEE Trans. Cybern.* **2024**, *early access*.
30. Huang, C.; Liu, Z.; Chen, C.P.; Zhang, Y. Adaptive fixed-time neural control for uncertain nonlinear multiagent systems. *IEEE Trans. Neural Netw. Learn. Syst.* **2022**, *34*, 10346–10358. [CrossRef]
31. Xu, B.; Liang, Y.; Li, Y.X.; Hou, Z. Adaptive command filtered fixed-time control of nonlinear systems with input quantization. *Appl. Math. Comput.* **2022**, *427*, 127186. [CrossRef]
32. Wang, H.; Shen, L. Adaptive fuzzy fixed-time tracking control for nonlinear systems with time-varying full-state constraints and actuator hysteresis. *IEEE Trans. Fuzzy Syst.* **2022**, *31*, 1352–1361. [CrossRef]
33. Liu, W.; Ma, Q.; Xu, S. Fuzzy fixed-time prescribed-performance tracking control of nonlinear systems with dynamic event-triggered signal. *IEEE Trans. Fuzzy Syst.* **2023**, *32*, 1399–1408. [CrossRef]
34. Wang, C.; Wang, J.; Du, Y.; Zhang, C.; Liu, Z.; Chen, C.P. Fixed-time event-triggered fuzzy adaptive control for uncertain nonlinear systems with full-state constraints. *Inf. Sci.* **2023**, *633*, 158–169. [CrossRef]
35. Liu, Y.; Liu, X.; Jing, Y. Adaptive neural networks finite-time tracking control for non-strict feedback systems via prescribed performance. *Inf. Sci.* **2018**, *468*, 29–46. [CrossRef]
36. Kang, Z.; Shen, Q.; Wu, S.; Damaren, C.J. Prescribed performance-based fixed-time adaptive control allocation for overactuated spacecraft. *J. Guid. Control Dyn.* **2023**, *46*, 390–400. [CrossRef]
37. Gao, Z.; Zhang, Y.; Guo, G. Fixed-time prescribed performance adaptive fixed-time sliding mode control for vehicular platoons with actuator saturation. *IEEE Trans. Intell. Transp. Syst.* **2022**, *23*, 24176–24189. [CrossRef]
38. Su, Y.; Xue, H.; Wang, Y.; Pan, Y. Command filter-based event-triggered adaptive fixed-time output-feedback control for large-scale nonlinear systems. *Int. J. Syst. Sci.* **2021**, *52*, 3190–3205. [CrossRef]
39. Sun, W.; Yuan, J.; Yang, X. Fixed-time prescribed performance control method for nonlinear systems with unknown time-varying parameters. *IET Control Theory Appl.* **2024**, *18*, 1751–1762. [CrossRef]
40. Wang, N.; Wang, Y. Fuzzy adaptive quantized tracking control of switched high-order nonlinear systems: A new fixed-time prescribed performance method. *IEEE Trans. Circuits Syst. II* **2022**, *69*, 3279–3283. [CrossRef]
41. Hua, Z. Fixed-time prescribed performance tracking for nonlinear systems with unknown time-varying input delay. *Nonlinear Dyn.* **2025**, *113*, 661–680. [CrossRef]
42. Li, T.; Zhang, J.; Li, S.; Zhou, P.; Lv, D. Neural-based adaptive fixed-time prescribed performance control for the flexible-joint robot with actuator failures. *Nonlinear Dyn.* **2023**, *111*, 16187–16214. [CrossRef]
43. Zhang, Y.; Liu, Z.; Wang, F.; Chen, Z. Distributed power allocation scheme with prescribed performance and intermittent dynamics for BESSs with discharge rate constraints in microgrids. *IEEE Trans. Syst. Man Cybern. Syst.* **2024**, *55*, 1948–1959. [CrossRef]
44. Chen, Q.; Wu, L.B.; Chen, M.; Liu, M.R. Fixed-time adaptive event-triggered fault-tolerant control of nonlinear systems with actuator failures. *Asian J. Control* **2025**, *27*, 765–781. [CrossRef]
45. Song, J.; Chen, Y.; Liu, Y.; Zhang, L. Fixed-time fuzzy adaptive fault-tolerant control for strict-feedback nonlinear systems with input delay. *IEEE Trans. Syst. Man. Cybern. Syst.* **2023**, *53*, 6999–7010. [CrossRef]
46. Chen, Q.; Wu, L.B. Fixed-time adaptive fault-tolerant control of stochastic nonlinear systems with time-varying full-state constraints. *Nonlinear Dyn.* **2024**, *112*, 22113–22129. [CrossRef]
47. Mei, Y.; Wang, J.; Park, J.H.; Shi, K.; Shen, H. Adaptive fixed-time control for nonlinear systems against time-varying actuator faults. *Nonlinear Dyn.* **2022**, *107*, 3629–3640. [CrossRef]
48. Wang, H.; Ma, J.; Zhao, X.; Niu, B.; Chen, M.; Wang, W. Adaptive fuzzy fixed-time control for high-order nonlinear systems with sensor and actuator faults. *IEEE Trans. Fuzzy Syst.* **2023**, *31*, 2658–2668. [CrossRef]
49. Liu, R.; Liu, M.; Ye, D.; Yu, Y. Event-triggered adaptive fixed-time fuzzy control for uncertain nonlinear systems with unknown actuator faults. *Inf. Sci.* **2022**, *612*, 344–360. [CrossRef]
50. Zhang, X.; Tan, J.; Wu, J.; Chen, W. Event-triggered-based fixed-time adaptive neural fault-tolerant control for stochastic nonlinear systems under actuator and sensor faults. *Nonlinear Dyn.* **2022**, *108*, 2279–2296. [CrossRef]

51. Wang, C.; Shi, Y. Fixed-time fuzzy adaptive tracking control of full-state constrained nonlinear systems with unknown virtual control coefficients. *Int. J. Fuzzy Syst.* **2024**, *26*, 196–211. [CrossRef]
52. Ma, J.; Park, J.H.; Xu, S. Command-filter-based finite-time adaptive control for nonlinear systems with quantized input. *IEEE Trans. Autom. Control* **2020**, *66*, 2339–2344. [CrossRef]